Molecular Crystals and Liquid Crystals Science and Technology. Section A. Molecular Crystals and Liquid Crystals
Publication details, including instructions for authors and subscription information:
http://www.tandfonline.com/loi/gmcl19

Rheological and Physical Properties of Liquid Crystalline Polymer Blends

Byoung Chul Kim [a] & Soon Man Hong [a]
[a] Division of Polymer Researches, Korea Institute of Science and Technology, P.O. Box 131, Cheongryang, Seoul, Korea
Version of record first published: 24 Sep 2006.

To cite this article: Byoung Chul Kim & Soon Man Hong (1994): Rheological and Physical Properties of Liquid Crystalline Polymer Blends, Molecular Crystals and Liquid Crystals Science and Technology. Section A. Molecular Crystals and Liquid Crystals, 254:1, 251-265

To link to this article: http://dx.doi.org/10.1080/10587259408036080

Mol. Cryst. Liq. Cryst. 1994, Vol. 254, pp. 251–265
Reprints available directly from the publisher
Photocopying permitted by license only

Printed in the United States of America

RHEOLOGICAL AND PHYSICAL PROPERTIES OF LIQUID CRYSTALLINE POLYMER BLENDS

BYOUNG CHUL KIM and SOON MAN HONG
Division of Polymer Researches, Korea Institute of Science and Technology, P.O. Box 131 Cheongryang, Seoul, Korea

(Received: February 7, 1994)

Abstract The binary and ternary blends consisting of an isotropic polymer and a thermotropic liquid crystalline polymer (LCP) were investigated in terms of rheology, morphology, and physical properties. In the binary blends, Vectra A950 lowered the melt viscosity of polyarylate (PAR), and Vectra B950 promoted the crystallization of polyphenylenesulfide (PPS). Introducing a third component into these binary blends, a multiblock copolyesterether into the PAR/Vectra A950 blends and a polysulfone into the PPS/Vectra B950 blends, helped elongate the dispersed LCP domains and enhanced the interface adhesion. The ternary LCP blends produced *in-situ* composites with improved mechanical properties.

INTRODUCTION

It has been a subject of significant commercial importance for most polymer engineers to obtain polymeric materials with desired physical properties to meet diverse requirements of industrial appications. Several suggested methods include molecular design of new class polymers, blending and alloying of different polymers, and incorporation of inorganic materials into polymers.

It would be highly desirable to find an approach in which the self-reinforcement is accomplished during the fabrication process. Melt blending of incompatible isotropic polymer and thermotropic liquid

crystalline polymer (LCP) produces a composite in which fibrous LCP domains play a role of reinforcement in the isopropic matrix polymer, because the molten LCP at the processing temperature comes out as elongated crystals with cooling. Thus, the *in-situ* formation of the reinforcing species during the fabrication process leads to the term *in-situ* composite[1,2]. Some fascinating merits of the *in-situ* composite over the inorganic reinforced thermoplastic composite are lower melt viscosity, finer dispersion of reinforcing materials, less equipment abrasion, and easier control of detrimental mechanical properties originating from different thermal expansion coefficients between organic matrix polymer and inorganic reinforcement.

A number of papers on the LCP blends with isotropic polymer have been published during the last decade. Most of them deal with binary *in-situ* composites prepared from melt blending a LCP and an isotropic polymer. These binary *in-situ* composites, however, frequently give rise to unsatisfactory mechanical properties because of phase separation and poor interface contact. We have attempted to overcome these shortcomings by incorporating an appropriate third polymeric component into the binary LCP blends. After investigating the two binary blend systems, polyarylate/Vectra A950 and polyphenylenesulfide/Vectra B950, the effect of incorporating a third component, Hytrel 7246 and polysulfone, into these binary blends has been studied.

EXPERIMENTAL

As matrix polymer, a commercial grade polyarylate U-Polymer 100 (PAR) of Unitika and a polyphenylenesulfide Ryton GR-02 (PPS) of Phillips Petroleum were used. The reinforcing components were commercial grade thermotropic copolyester Vectra A950 (LCP-1) and Vectra B950 (LCP-2) of Hoechst-Celanese. As third component, an Amoco polysulfone Udel P-1700 (PSF) and a Du Pont multiblock copolyesterether Hytrel 7246 (CEE) were tested for PPS/LCP-2 and PAR/LCP-1 blends, respectively. The materials were dried in a forced convection oven overnight before use.

The formulated components were compounded in a Brabender twin-screw extruder in the nitrogen atmosphere. The specimen for rheological measurements were prepared by compression molding to minimize the residual stress. The dynamic rheological properties were

measured by Rheometrics dynamic spectrometer RDS-7700 with the concentric parallel plates. In the RDS measurements, the diameter of the plates was 25mm and the gap size was 1.5mm.

The thermal properties were measured with a Du Pont Thermal Analysis 2000 equipped with a 910 DSC. The DSC measurements were carried out in the nitrogen atomosphere with a scan rate of 10°C/min. The DSC thermogram was obtained during the second heating stage to obtain more consistent data. The isothermal crystallization behavior of PPS was observed by heating the sample up to 330°C under nitrogen gas, holding for 3min at 330°C, and then quenching at the rate of 160°C/min to a predetermined crystallization temperature at which the exothermic crystallization peak was recorded. The nonisothermal crystallization behavior was observed at a constant cooling rate (2, 4, 8, and 12°C/min), immediately after 3 min's holding at 330°C.

The spinning experiments were carried out using a spinning capillary die attached to the twin-screw extruder, whose radius and length were 2 and 20mm, respectively. The strand leaving the die exit was directly quenched in a water bath and drawn with a take-up machine. To examine the morphology, the blend fibers were embedded in an epoxy resin and fractured in the liquid nitrogen. The fractured surface was observed by Hitatchi scanning electron microscope S-510. The orientation was determined from the wide angle X-ray spectra of the blend fiber bundles obtained by Rigaku D/Max X-ray diffractometer. The tensile properties were measured by Instron tensile tester 4201 with adopting gauge length 30mm and crosshead speed 5mm/min.

RESULTS AND DISCUSSION

PAR/LCP-1 Blend Systems

DSC thermograms of the PAR/LCP-1 blends are shown in Fig.1. The amorphous PAR clearly exhibits a composition independent glass transition (T_g) in the vicinity of 191°C, and LCP shows a weak endothermic peak at 279°C indicating a transition from crystalline phase to nematic mesophase (T_{cn}). This indicates that PAR and LCP are incompatible over the blending ratios examined. A careful observation of the phase morphology with time examined by polarizing microscope equipped with a hot stage excludes the possibility of the transesterification reaction between PAR and LCP during the melt

processing[3].

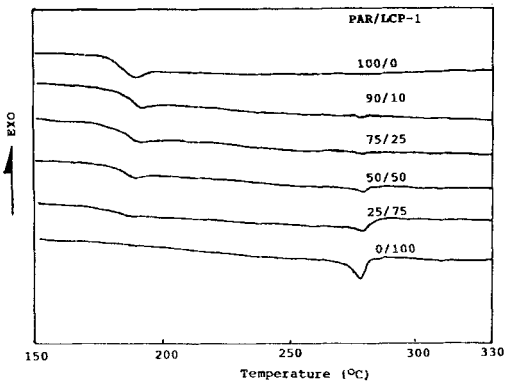

Fig.1. DSC thermograms of PAR/LCP-1 blends at the heating rate of 10°C.

In the case of LCP, most of the orientation and texture generated during the fabrication process are maintained into the final solid product. Consequently it is very important to understand the rheological behavior of LCP for the precise control of resultant morphology. However, a number of fundamental questions about the measuring procedure and interpretating the results have remained unsolved on account of unusually high sensitivity of LCP to thermal and shear histories[4-6]. Similar problems are also true for the polymer blends containing LCP. In this study, the rheological properties are provided only to assess the practical processability and processing characteristics of the LCP blends in a macroscopic way.

The viscosity curves of PAR/LCP blends are shown in Fig.2. Pure PAR and PAR/LCP blends containing LCP less than 25wt% exhibit viscosity curves typical of ordinary thermoplastics, while the flow properties of PAR/LCP blends containing LCP more than 50wt% are greatly affected by the LCP phase[7,8]. The disappearance of Newtonian flow region at low shear rates in the viscosity curves of pure LCP and LCP rich blends indicates an existence of non-zero yield stress necessary to initiate flow. That is, the blend systems are heterogeneous possibly due to the presence of anisotropic solids of LCP.

The melt viscosity of the blends at 280°C is increased with increasing the LCP content whereas LCP lowers the melt viscosity of PAR over the entire frequency range tested at 300°C. This suggests that LCP plays a role of a processing aid for the highly viscous PAR melt at 300°C. A possible morphological change with increasing the melt

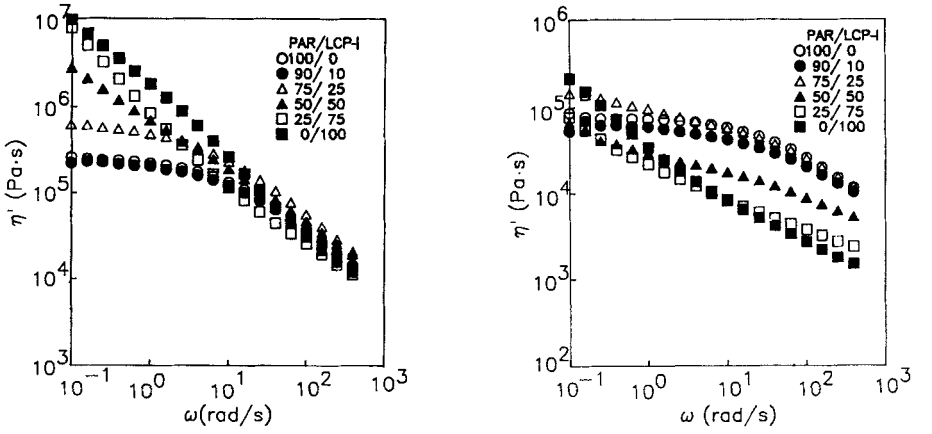

(a) at 280°C (b) at 300°C

Fig.2. Viscosity curve of PAR/LCP-1 blends.

temperature is supposed to be a gradual disappearance of anisotropic LCP independent of temperature, more obviously in the PAR rich blends as shown in Fig.3. In addition, incorporating LCP shifts the plot to higher

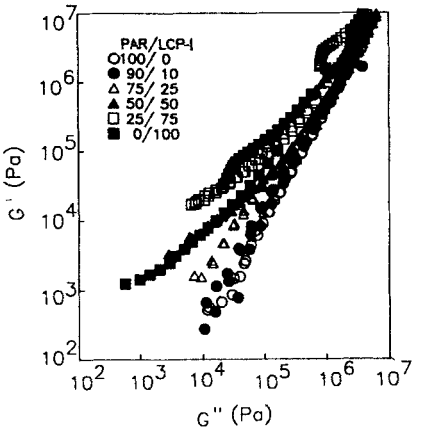

Fig.3. Plot of storage modulus (G′) of PAR/LCP-1 blends vs. loss modulus (G″) at 280 and 300°C.

G values and decreases the slope of the plot, which has been usually reported to be 2 for most flexible chain polymers. This indicates that homogeneous PAR becomes heterogeneous through phase separation with increasing the LCP content.

The tensile strength of PAR/LCP fibers drawn at 300 and 340°C with varying composition is given in Fig.4. An increase of LCP content

and spin draw ratio increase the tensile strength of the blend fibers. Further, the increase in tensile strength with increasing spin draw ratio is more prominent with the LCP rich blend fiber. It is worth noting that spinning temperature has a noticeable effect on the mechanical performance of resultant bicomponent fibers. Fibers spun at 300°C exhibit greater tensile strength than those spun at 340°C, particularly in the LCP rich blend fibers. Rheologically speaking, two things are important to produce greater elongation of dispersed phase; the relative viscosity of the matrix should be larger than the dispersed phase and the viscosity ratio of two phases should be close to unity[11-13]. The viscosity

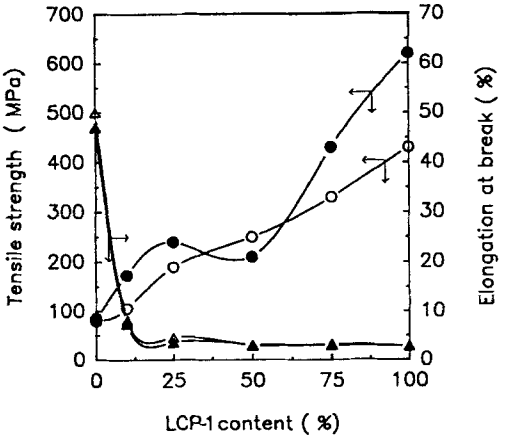

Fig.4. Tensile strength and elongation at break vs. the LCP-1 content for PAR/LCP-1 fibers at a draw ratio 4: spun at 300°C (open symbols) and at 340°C (closed symbols).

ratio of PAR to LCP melts over the frequency range from 1 to 400rad/sec is measured to be 2 to 9 at 300°C and 13 to 28 at 340°C. Thus, the better dispersion and increased aspect ratio of fibrillar LCP domains are the reason for the better mechanical properties of blend fibers spun at 300°C than those spun at 340°C. The microstructure shown in Fig.5 firmly ascertains this. The reduction of draw resonance is an additional reason, particularly in the LCP rich blend fibers.

PAR/LCP-1/CEE Blend Systems

Fig.6 shows the effect of CEE on the rheological properties of 50/50 PAR/CEE blend. An increase of the CEE content reduces both viscosity and elasticity. However, the blend including 2phr CEE exhibits higher viscosity and elasticity than that with 1phr CEE. This implies that less free volume between PAR and LCP melts and better mixing result at the CEE level of ca. 2phr[14].

Introducing CEE increases the minimum tensile strength of

PAR/LCP-1 blend usually observed at the blend ratio 50/50 as shown in Fig.7. The optimum usage level of CEE proves to be ca. 2phr, which coincides with the rheological prediction. When 2phr of CEE is added to

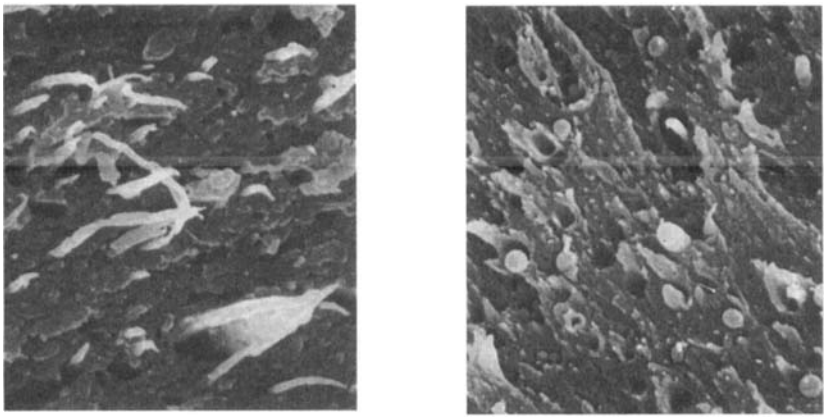

(a) at 300°C (b) at 340°C

Fig.5. SEM photomicrographs of tensiled fractured surface of 90/10 PAR/LCP-1 as-spun fibers at a draw ratio 4, spun at two different temperatures.

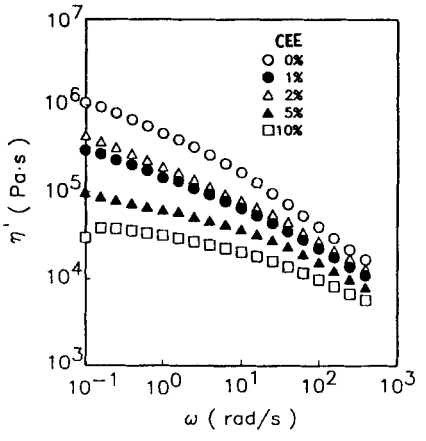

Fig.6. Viscosity curve of PAR/LCP-1/CEE blend at 280°C.

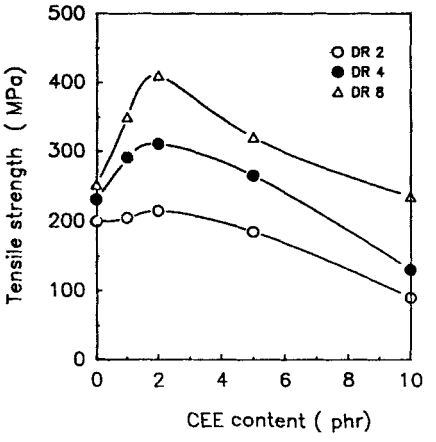

Fig.7. Effect of CEE on the tensile strength of PAR/LCP-1/CEE fiber spun at 300°C.

the PAR/LCP-1 blend, the tensile fractured morphology of the blend fiber in Fig.8 reveals that a filament is divided into many macro/micro fibrils. However, blend fibers containing 5 to 10phr of CEE give rise to a brittle fracture. This fractured structure also suggests that the enhanced mechanical properties by incorporating CEE come from the reduced free volume between PAR and LCP phases through improved interface adhesion and more homogeneous mixing.

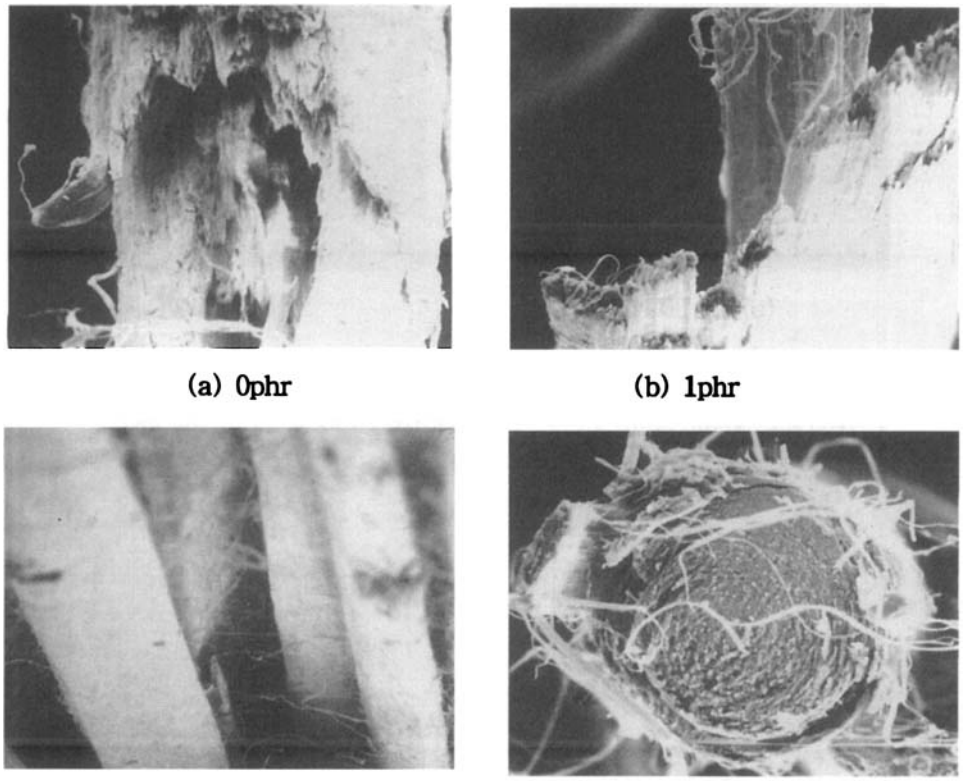

(a) 0phr (b) 1phr

(c) 2phr (d) 5phr

Fig.8. SEM photomicrographs of tensile fractured surface of 50/50 PAR/LCP-1 fibers spun at 300°C with varying the CEE content.

PPS/LCP-2 Blend Systems

DSC thermograms of PPS/LCP-2 blend systems are shown in Fig.9. The pure PPS exhibits T_g at 90°C, a broad T_m peak at 279°C, a cold exotherm crystallization peak (T_{cc}) at 119°C, and a melt crystallization peak (T_{mc}) at 206°C. The pure LCP-2 exhibits T_{cn} at 282°C. It should

be noted in Fig.9 that all the thermal transitions of PPS remain almost unchanged with increasing the LCP content, which verifies that the two polymers are incompatible over all the blending compositions examined[15].

The isothermal crystallization kinetics of pure PPS and PPS/LCP-2 blend systems is analyzed on the basis of the DSC thermograms. The crystallization half-time ($t_{1/2}$; the time at which the extent of crystallization is 50% complete) is plotted against the isothermal crystallization temperature (T_{ic}) in Fig.10. Like other semicrystalline polymers the $t_{1/2}$ is generally increased with increasing T_{ic}. An inclusion of LCP dramatically decreases the $t_{1/2}$, particularly at lower crystallization

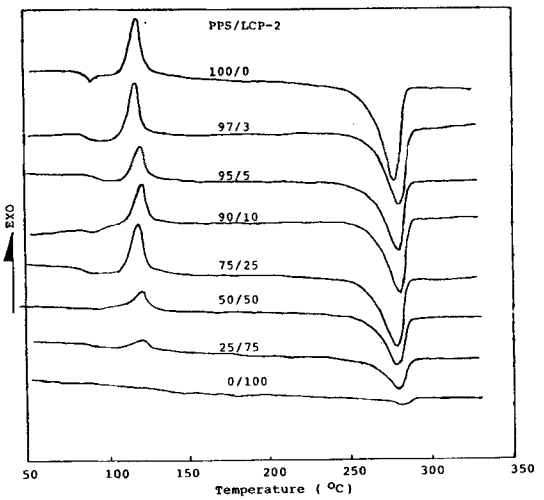

Fig.9. DSC thermogram of PPS/LCP-2 blends at the heating rate of 10°C.

process of PPS, resulting in a heterogeneous nucleation. The polarized optical micrographs show that the pure PPS gives larger spherulites whereas the LCP filled PPS produces fine grain spherulitic structures[15]. In general, the nucleation density of PPS and LCP filled PPS is decreased with increasing the crystallization temperature as shown in Fig.11. According to the thermal analysis of Lopez[17], the thermodynamic equilibrium melting temperature of pure PPS is about 312°C, at which perfect crystals of infinite size melt. This raises a possibility of the presence of some unmelted crystals and metastable nuclei below 312°C, which promote nucleation[15,16]. Thus over the temperature range, 230 to 255°C, the number of metastable PPS nuclei is decreased as temperature is increased. In consequence, with increasing the temperature, the nucleation density is diminished and larger spherulites result.

Viscosity behavior of pure PPS and PPS/LCP-2 blend systems is

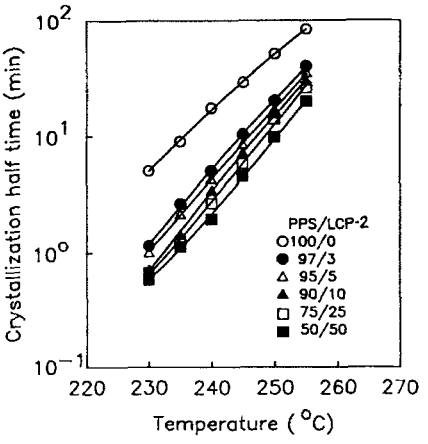

Fig.10. Crystallization half time vs. isothermal crystallization temperature for various PPS/LCP-2 blends.

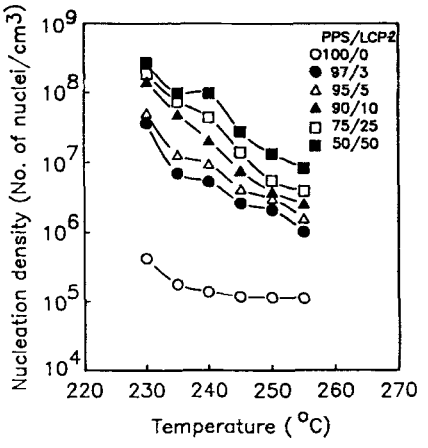

Fig.11. Nucleation density vs. crystallization temperature for various PPS/LCP-2 blends.

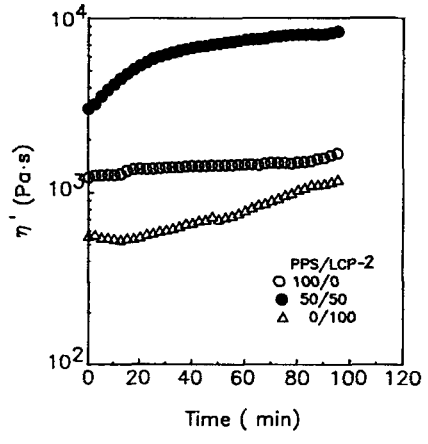

Fig.12. Time dependence of viscosity of PPS/LCP-2 blends at 290°C.

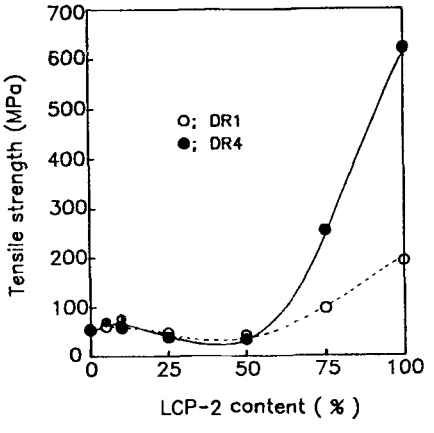

Fig.13. Tensile strength of PPS/LCP-2 fibers spun at 290°C.

very complicated[15]. Further, it exhibits a time dependence as shown in Fig.12. The increase of viscosity with time is attributable to dual characteristics of thermoplastic and thermoset of PPS. Because of the similar reasons with the PAR/LCP-1 blend systems, plotting G′ of

PPS/LCP-2 blend systems against G″ instead of frequency eliminates the effect of temperature and incorporating LCP reduces the slope of the plot[15].

Fig.14 presents the variation of the tensile strength of the as-spun PPS/LCP-2 fibers with the LCP-2 content. The blend fiber gives tensile strength falling below that predicted by the additivity rule. Further, the tensile strength gives a minimum value in the vicinity of the blending ratio PPS/LCP 50/50. Similar results for other LCP blend systems have also been reported[20,21]. They have attributed it to cleavage, cavitation, interfacial debonding, poor dispersion and destruction of heterogeneities resulting from the phase separation by crystallization between two immiscible polymers. The effect of drawing on the ultimate tensile strength is more noticeable in the LCP rich blend fibers than in the PPS

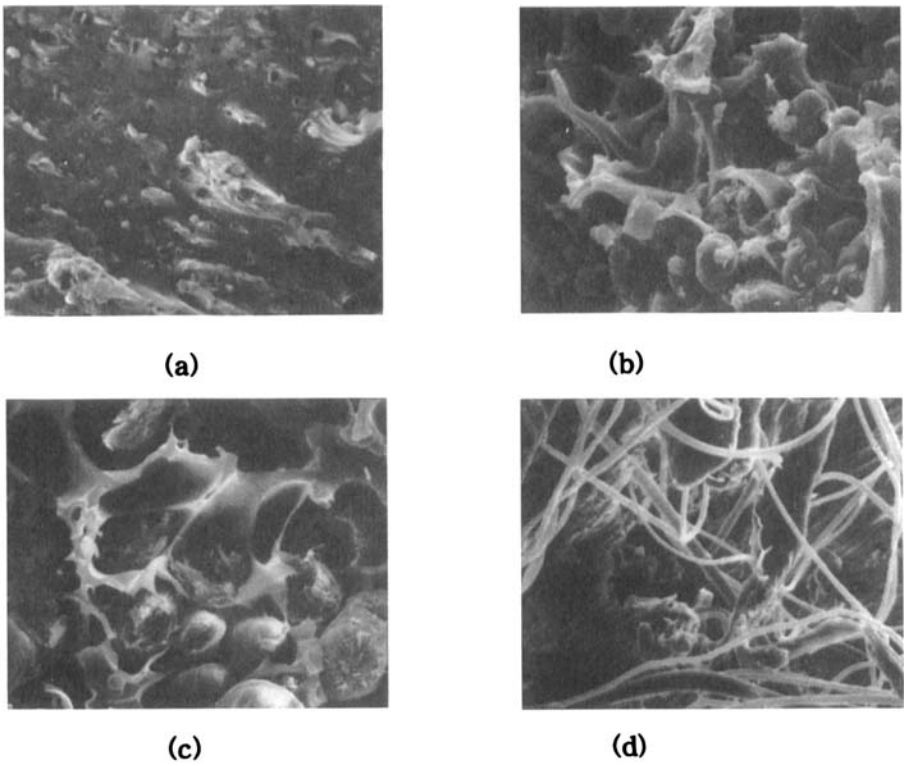

Fig.14. SEM photomicrographs of tensiled fractured surface of PPS/LCP-2 fibers at a draw ratio of 8: (a) PPS/LCP-2=95/5, (b) 75/25, (c) 50/50, and (d) 25/75.

rich blend fibers as can be predicted.

An observation of the microstructure of the PPS/LCP-2 blend systems in Fig.14 reveals that a phase separation occurs regardless of the blend composition. In addition, the LCP component is dispersed as droplet domains in the PPS phase up to the LCP content of 50wt%, but further increasing the LCP content develops a fiberlike orientation. Especially with increasing the LCP content up to 50wt% the spherical domain size is increased in the dimensions of order of 20 to 30μm owing to the aggregation of the droplets in the molten state. On the whole, a rather heterogeneous size distribution is noticed and most particles remain in spherical or ellipsoidal shape. This is obliged to the fact that the viscosity of the matrix PPS is too low to deform and break the spherical particles of the dispersed LCP domains[22].

PPS/LCP-2/PSF Blend Systems

As mentioned in the previous section, the viscosity of PPS is too low to deform and break dispersed LCP domains during elongational flow at the spinning temperature 300°C. Fig.15 shows the effect of PSF on the rheological properties of PPS/LCP-2 blends containing 10phr LCP. In these blends, PSF increases the viscosity of PPS, which allows the load transfer from the matrix to the dispersed phase easier and hence

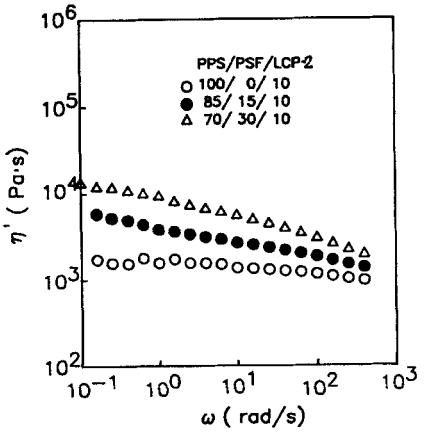

Fig.15. Viscosity curve of PPS/LCP-2/PSF blends at 290°C.

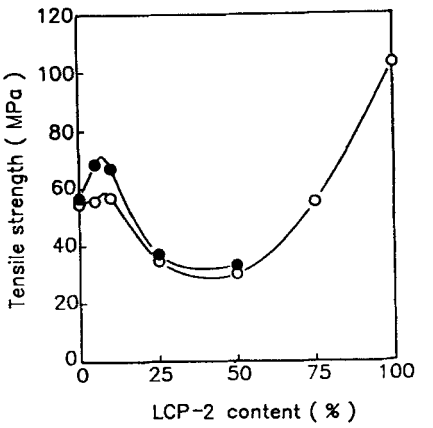

Fig.16. Tensile strength of injection-molded blend plagues: O; without PSF and O; with 30phr PSF.

increases the aspect ratio of dispersed LCP domains[23].

Addition of PSF in the PPS system may also expect some degree of chemical interactions because both polymers are aromatic and contain sulphur, as recently reported by several researchers[20,21]. According to their results in the 70/30 PPS/PSF blend the PSF phase is dispersed as spherical particles of dimensions about 1-5μm in a continuous PPS matrix, and the tensile strength and Young's modulus of the blends are roughly constant. However, addition of PSF as a third tie resin on the PPS/LCP blends enhances the tensile properties as shown in Fig.16. Two principal reasons may be given to explain the improved mechanical properties. Firstly, the flexible amorphous PSF reduces the free volume at the interface of the crystalline polymers in the blends. Secondly, the PSF with higher viscosity facilitates the fibril formation and the molecular orientation of LCP under shearing. The latter is clearly

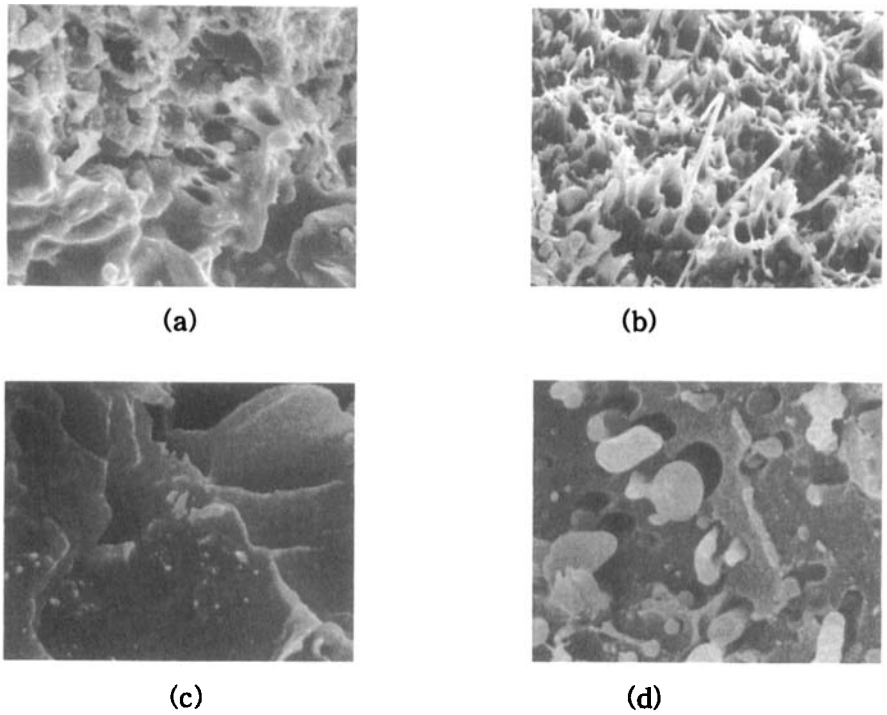

Fig.17. SEM photomicrographs of tensile fractured surface of ternary fibers and injection-molded plagues, demonstrating the effect of incorporating 30wt% PSF to the binary 90/10 PPS/LCP-2 blend: (a) and (b) exhibit fibers with and without PSF, and (c) and (d), plagues with and without PSF, respectively.

illustrated by SEM photomicrographs of the fractured surface of the injection-molded parts and as-spun fibers of ternary PPS/LCP-2/PSF blend systems in Fig.17. The spherical or ellipsoidal LCP domains are deformed into rod-like or thread-like fibrils by introducing PSF to the PPS/LCP blends.

CONCLUSION

Introducing a suitable third polymeric component into the binary LCP blends has turned out to be effective in enhancing the dispersion and stretching of LCP domains within the isotropic matrix polymer. Further, it improves the interface contact between reinforcing LCP and isotropic matrix polymer in the resultant *in-situ* composite. This ternary LCP blend concept possesses a strong potential for manufacturing *in-situ* composites with a high mechanical performance.

REFERENCES

1. J.L. Kardos, W.L. McDonnel, and J. Raisoni, *J. Macromol. Sci. Phys.*, B6, 397 (1972).
2. G. Kiss, *Polym. Eng. Sci.*, 27, 410 (1987).
3. S.M. Hong, B.C. Kim, S.S. Hwang, and K.U. Kim, *Polym. Eng. Sci.*, 33, 630 (1993).
4. R.S. Irwin, W. Sweeny, K.H. Gardner, C.R. Gochanour, and M. Weinberg, *Macromolecules*, 22, 1065 (1989).
5. J. Nam, T. Fukai, and T. Kyu, *Macromolecules*, 24, 6250 (1991).
6. S.S. Kim and C.D. Han, *Macromolecules*, 26, 3176 (1993).
7. K.F. Wissbrun, *J. Rheol.*, 25, 619 (1981).
8. K.F. Wissbrun, *Brit. Polym. J.*, Dec., 163 (1980).
9. R.M. Ottenbrite, L.A. Utracki, and S. Inoue, "*Current Topics in Polymer Science*", Vol.II, pp. 149-165, Hanser Publisher, Munichi, 1987.
10. C.D. Han and J.H. Kim, *J. Polym. Sci.*, Part B25, 1741 (1987).
11. K.G. Blizard and D.G. Baird, *Polym. Eng. Sci.*, 27, 653 (1987).
12. D. Acierno, E. Amendola, L. Nicolais, and R. Nobile, *Mol. Cryst. Liq. Cryst.*, 153, 553 (1987).
13. M.R. Nobile, E. Amendola, L. Nicolais, D. Acierno, and C. Carfagna,

Polym. Eng. Sci., 29, 224 (1989).
14. S.M. Hong and B.C. Kim, *Polym. Eng. Sci.*, (in press).
15. S.M. Hong, B.C. Kim, K.U. Kim, and I.J. Chung, *Polym. J.*, 24, 727 (1992).
16. S.H. Jung, PhD. Dissertation, KAIST (1988).
17. L.C. Lopez and G.L. Wilkes, *Polymer*, 29 106 (1988).
18. S. Kumar, D.P. Anderson, and W.W. Adams, *Polymer*, 27, 329 (1986).
19. F. Rybnikar, *J. Appl. Polym. Sci.*, 27, 1479 (1982).
20. M.F. Cheung, A. Golovoy, H.K. Plummer, and H.V. Oene, *Polymer*, 31, 2299 (1990).
21. S. Akhtar and J.L. White, *Polym. Eng. Sci.*, 31, 84 (1991).
22. H.B. Chin and C.D. Han, *J. Rheol.*, 23, 557 (1979).
23. B.C. Kim, S.M. Hong, and K.U. Kim, *Polym. Eng. Sci.*, (submitted).